Coronin 2A regulates a subset of focal-adhesion-turnover events through the cofilin pathway

Thomas W. Marshall, Heather L. Aloor and James E. Bear*

Lineberger Comprehensive Cancer Center and Department of Cell and Developmental Biology, University of North Carolina-Chapel Hill, Chapel Hill, NC 27599, USA

*Author for correspondence (jbear@email.unc.edu)

Accepted 27 May 2009
Journal of Cell Science 122, 3061-3069 Published by The Company of Biologists 2009
doi:10.1242/jcs.051482

Summary

Coronins are conserved F-actin-binding proteins that are important for motility and actin dynamics. Unlike type I coronins, coronin 2A localizes to stress fibers and some focal adhesions, and is excluded from the leading edge. Depletion of coronin 2A in MTLn3 cells decreases cell motility and turnover of focal adhesions. Surprisingly, none of the pathways known to regulate focal-adhesion turnover are affected by depletion of coronin 2A. Depletion of coronin 2A does, however, increase phospho-cofilin, suggesting that misregulation of cofilin might affect adhesion dynamics. Slingshot-1L, a cofilin-activating phosphatase, localizes to focal adhesions and interacts with coronin 2A. Depletion of coronin 2A reduces cofilin activity at focal adhesions, as measured by barbed-end density and actin FRAP. In both fixed cells and live cells, cofilin localizes to the proximal end of some focal adhesions. Although expression of wild-type cofilin in coronin-2A-depleted cells has no major effect on focal-adhesion dynamics, expression of an active mutant of cofilin bypasses the defects in cell motility and focal-adhesion disassembly. These results implicate both coronin 2A and cofilin as factors that can regulate a subset of focal-adhesion-turnover events.

Supplementary material available online at
http://jcs.biologists.org/cgi/content/full/122/17/3061/DC1

Key words: Coronin, Cofilin, Slingshot

Introduction

Precise control of cell-matrix adhesion is necessary for cell migration to occur. Fibroblasts lacking paxillin (PXN) or focal adhesion kinase (FAK), two core focal-adhesion components, display aberrant adhesion and decreased cell motility in vitro. Embryos deficient in genes that encode these proteins also lack proper mesoderm formation leading to embryonic lethality (Ilic et al., 1995; Hagel et al., 2002). In many types of cancer cell, focal adhesion proteins display either modulated protein expression or inappropriate regulation. For example, FAK is overexpressed in many types of cancer cells and is responsible for hyper-phosphorylation of other focal-adhesion proteins (Mitra and Schlaepfer, 2006). Conversely, targeted disruption of the FAK gene in breast cancer models show that FAK is required for carcinoma formation and metastasis (Lahlou et al., 2007). Other focal-adhesion proteins have altered expression profiles in cancer models as well. Recent data suggest that the EGF-induced switch from expression of tensin-3 to the expression of the anti-adhesive molecule cten leads to increased metastasis of mammary tumor cells (Katz et al., 2007). These observations indicate that proper focal-adhesion dynamics are crucial for morphogenesis and play a significant role in cancer progression.

Coronins are highly conserved F-actin binding proteins that are important for cell motility and actin dynamics (de Hostos et al., 1993; Cai et al., 2007; Foger et al., 2006). Mammalian genomes contain at least six coronin genes that can be separated into three types: type I (coronin 1A, 1B and 1C), type II (coronin 2A and 2B), and type III (coronin 7, also known as POD) (Uetrecht and Bear, 2006). Each of the coronins displays different tissue expression patterns with at least one type I coronin and POD expressed in all tissues and cell types. Type II coronins show a more restricted expression pattern, with strong enrichment in tissues containing epithelial and neuronal cell types (Cai et al., 2005).

The subcellular localization of each of the coronin types is also quite distinct. Type I coronins localize primarily to the lamellipodia and some vesicular structures (Cai et al., 2005; Rosentreter et al., 2007), type II coronins localize to stress fibers and focal adhesions (Nakamura et al., 1999), and POD localizes to the Golgi apparatus (Rybakin et al., 2004). Type I coronins have a clear role in regulating cell motility, whereas the function of type II coronins remains unknown. Type I coronins such as coronin 1B coordinately regulate Arp2/3 and cofilin activities in lamellipodia (Cai et al., 2007). Coronin 1B targets Arp2/3-containing branches and replaces Arp2/3 at branches, leading to network remodeling and disassembly (Cai et al., 2008). In addition, coronin 1B is required for proper targeting of Slingshot-1L, an activating phosphatase for the ADF/cofilin family of actin-binding proteins to the rear of lamellipodia (Cai et al., 2007). It is unclear whether type II coronins execute similar functions at other cellular locations.

ADF/cofilin proteins (hereafter referred to as cofilin) promote actin dynamics by several mechanisms, including severing actin filaments (Bamburg and Bernstein, 2008). Depletion of cofilin by RNAi increases the thickness of stress fibers, decreases F-actin retrograde flow, and impairs whole-cell motility (Hotulainen et al., 2005; Sidani et al., 2007). Several pathways have been identified that regulate cofilin activity. Cofilin is inactivated by interacting with phosphatidylinositol (4,5)-bisphosphate on membranes (van Rheenen et al., 2007), by conformational changes induced by intracellular pH shifts (Frantz et al., 2008), or via phosphorylation of serine 3 by LIM kinase (LIMK) or TES kinase (TESK) (Yang et al., 1998; Toshima et al., 2001). All of these events prevent cofilin from binding to F-actin. Activation of cofilin can be achieved by

the dephosphorylation of serine 3 by the Slingshot and Chronophin phosphatases (Niwa et al., 2002; Gohla et al., 2005). Interestingly, both LIMK and Slingshot-1L share a common localization to focal adhesions (Foletta et al., 2004; Soosairajah et al., 2005). Despite the localization of these cofilin regulatory proteins to focal adhesions, cofilin activity has never been directly implicated in focal-adhesion dynamics.

Several mechanisms are known to regulate the disassembly of focal adhesions. These include microtubule targeting of focal adhesions (Kaverina et al., 1999), talin cleavage by calpain (Franco et al., 2004), changes in myosin-II-generated tension (Webb et al., 2004), and changes in FAK phosphorylation and interactions with dynamin (Ezratty et al., 2005). However, the inter-relationship among these mechanisms is poorly understood. An unexplored mechanism could involve cofilin-mediated actin-filament-severing activity at focal adhesions. Here, we have investigated the role of coronin 2A in regulating cofilin activity at focal adhesions and the subsequent effects on whole-cell motility.

Results

Coronin 2A localizes to stress fibers and focal adhesions, but not lamellipodia

To investigate the function of coronin 2A (also known as IR10, ClipinB, WDR2, coronin 4 and CRN5), we expressed coronin 2A tagged with GFP (Coro2A-GFP) in MTLn3 cells, a mammary adenocarcinoma cell line. Coro2A-GFP co-localizes along F-actin stress fibers and with vinculin at some focal adhesions (Fig. 1A). Interestingly, coronin 2A did not co-localize with coronin 1B (Fig. 1A) or coronin 1C (data not shown) at the leading edge of cells and was excluded from the lamellipodial region. These observations, along with the absence of type I coronins from focal adhesions (data not shown), indicate that type I and type II coronins have distinct properties that determine protein localization. Endogenous coronin 2A had the same localization pattern as Coro2A-GFP (Fig. 1B). Interestingly, coronin 2A only localizes to some of the internal focal adhesions that have stress fibers attached, but does not localize to focal complexes and adhesions found in the periphery of cells. Other focal-adhesion markers, such as talin and FAK, show similar partial co-localization with coronin 2A at internal focal adhesions (data not shown).

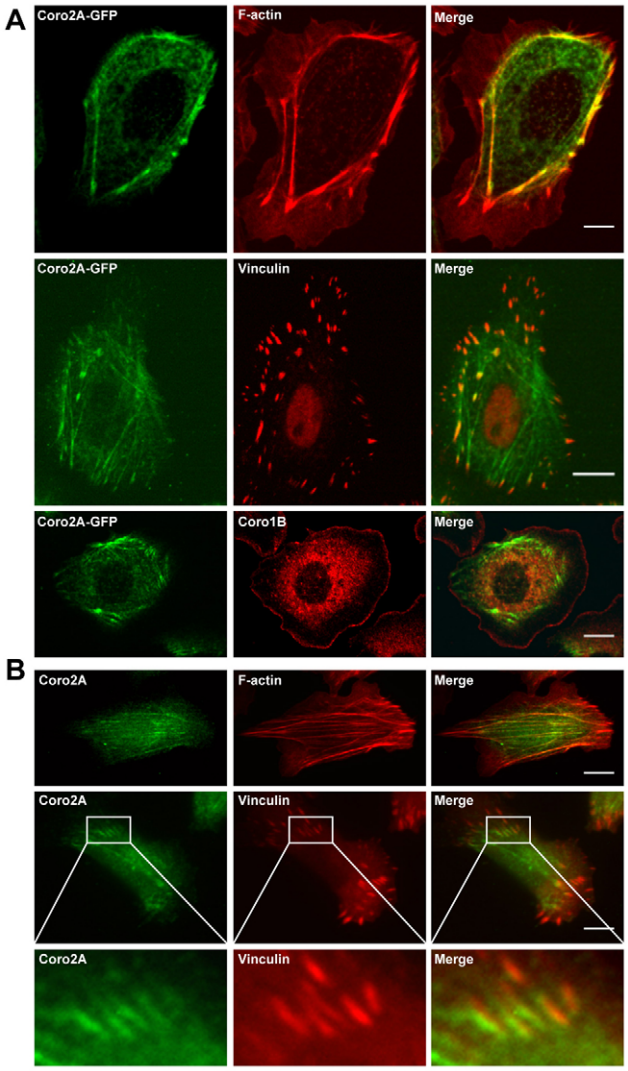

Fig. 1. Coronin 2A localizes to F-actin stress fibers and some focal adhesions, but is excluded from the leading edge. (A) MTLn3 cells expressing Coro2A-EGFP were stained with Alexa 568 phalloidin (top panel) or with antibodies against either vinculin (middle panel) or coronin 1B (bottom panel). (B) Immunofluorescence of endogenous coronin 2A (green) with either Alexa 568 phalloidin (top panel) or a vinculin antibody (middle panel). In the bottom panel, magnified images (6×) of the insets in the middle panels show that coronin 2A localizes to focal adhesions. Scale bars: 5 μm.

Coronin-2A-depleted cells display decreased cell speed, but show no change in lamellipodial dynamics

To address the functional role of coronin 2A, we developed an shRNA against rat coronin 2A (shCoro2A), delivered by lentivirus, to deplete this gene product. To control for the effects of lentiviral infection, we also used a non-specific shRNA (shNS). To verify that any effects were not due to off-target silencing, we developed a rescue construct that encodes both shCoro2A and an RNAi-resistant human coronin 2A tagged with GFP. Immunoblotting indicated that shCoro2A-expressing cells have nearly undetectable amounts of coronin 2A protein (Fig. 2A). This result was confirmed by qRT-PCR analysis (supplemental material Fig. S1A). Although cells expressing the rescue construct appeared to have levels of coronin 2A protein that were higher than endogenous levels, separate pilot experiments showed that this antibody recognizes human coronin 2A more strongly than rat coronin 2A (supplemental material Fig. S1B), indicating that the level of rescue protein expression was in the physiological range.

Since coronin 2A localizes to F-actin stress fibers and focal adhesions, we examined the motility of cells that were depleted of coronin 2A. Single-cell tracking indicated that coronin-2A-depleted cells have substantially reduced cell speed relative to control cells. Re-expression of human Coro2A-GFP restored cell speed to the level of control cells, indicating that the effects caused by the expression of shCoro2A are due to the specific depletion of coronin 2A (Fig. 2B). The cells depleted of coronin 2A displayed protrusion and retraction at the leading edge, but did not display much overall translocation. We used kymography to determine whether there were any differences in lamellipodial dynamics caused by the depletion of coronin 2A (example in Fig. 2C). Protrusion rate, protrusion distance, and persistence (Fig. 2D) were all unaffected by depletion of coronin 2A, suggesting that the decrease in cell motility is not due to alterations in lamellipodial dynamics.

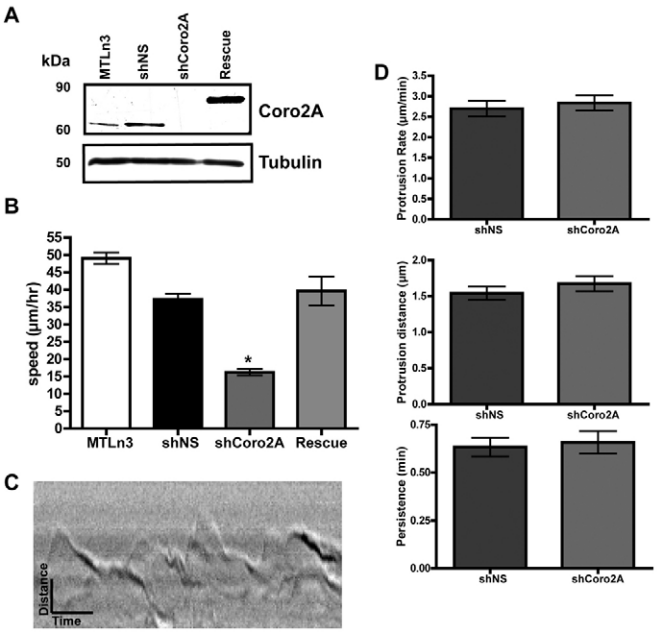

Fig. 2. Depletion of coronin 2A impairs cell motility, but does not affect lamellipodial dynamics. (A) MTLn3 cells were infected with lentivirus that expressed shRNAs against a non-specific sequence (shNS), coronin 2A (shCoro2A) or shCoro2A that also co-expressed human Coro2A-GFP (Rescue). Lysates were blotted for coronin 2A and for tubulin as a loading control. (B) Time-lapse microscopy of MTLn3, shNS, shCoro2A and Rescue cell lines was used to determine single-cell speed, depicted in graph. Error bars represent 95% confidence intervals. **P*<0.0001 by Student's *t*-test. See supplementary material Movie 1. (C) Representative kymograph of a protruding MTLn3 cell. (D) Protrusion rate, protrusion distance and persistence were calculated from the time (*y*-axis) and protrusion distance (*x*-axis) measured from kymographs. Error bars represent 95% confidence intervals.

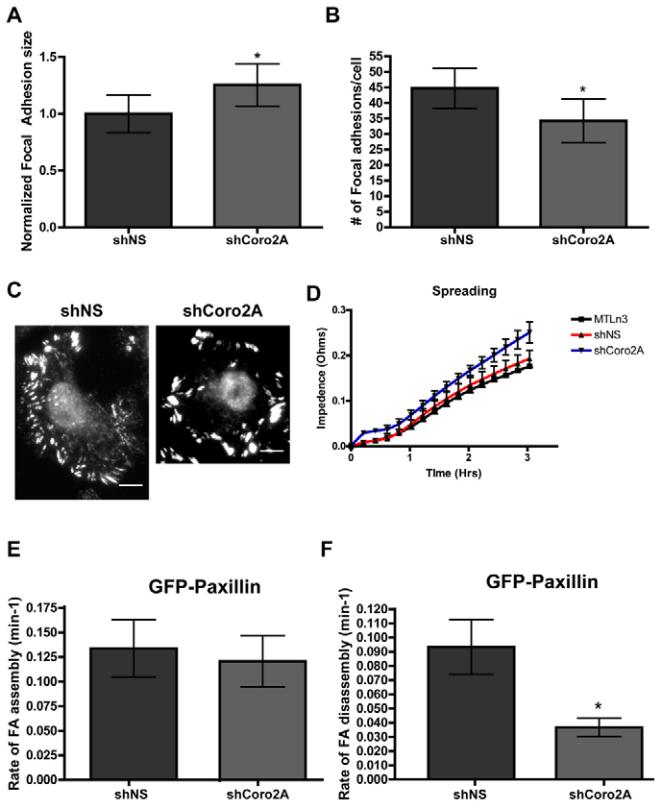

Fig. 3. Depletion of coronin 2A increases focal-adhesion size, decreases focal-adhesion number and decreases focal-adhesion disassembly. Focal-adhesion size (A) and number (B) were measured in MTLn3 cells expressing shNS or shCoro2A. Vinculin-positive focal adhesions were used for the quantifications. Focal-adhesion size was normalized against neighboring uninfected cells on the same coverslip. **P*=0.0424 for focal-adhesion size and **P*=0.0286 for focal-adhesion number, by Student's *t*-test. (C) Representative vinculin immunofluorescence for MTLn3 cells expressing shNS or shCoro2A used for quantifications in A and B. Scale bar: 5 μm. (D) Cell spreading as measured by change of impedance with the ACEA RT-CES system. Equal numbers of MTLn3, shNS and shCoro2A cells were plated in triplicate. *P*=0.1726 for MTLn3 versus shCoro2A and *P*=0.0661 for shNS versus shCoro2A, by Student's *t*-tests. (E,F) Average rates of focal-adhesion assembly (E) or disassembly (F) visualized by GFP-PXN in cells expressing either shNS or shCoro2A. Cells were imaged once a minute for 30 minutes (see supplementary material Movie 2). Changes of fluorescent intensity were used to determine focal-adhesion assembly and disassembly rates. **P*<0.001 by Student's *t*-test. Error bars represent 95% confidence intervals.

Cells depleted of coronin 2A have defects in focal-adhesion turnover

Since there are defects in cell motility in the coronin-2A-depleted cells and coronin 2A localizes to focal adhesions, the size and number of these structures were quantified. Quantification of focal adhesions in cells expressing either shNS or shCoro2A indicated that depletion of coronin 2A increases focal-adhesion size and decreases the total number of focal adhesions per cell (Fig. 3A,B, example images in C). To measure cell spreading, we used the ACEA RT-CES system that measures changes of impedance caused by cells interacting with a microelectrode within the surface of the dish. Coronin-2A-depleted cells showed a slight, but not statistically significant (*P*=0.1726 for MTLn3 versus shCoro2A, *P*=0.0661 for shNS versus shCoro2A) increase in cell spreading compared to control cells (Fig. 3D). This indicates that adhesion formation and cell spreading appear to be normal in coronin-2A-depleted cells.

Larger focal adhesions in the coronin-2A-depleted cells indicated that focal-adhesion dynamics might be affected. To investigate possible changes in focal-adhesion turnover, coronin-2A-depleted cells that co-express GFP-PXN were used to monitor focal-adhesion assembly and disassembly (Webb et al., 2004). Since coronin 2A is localized to a subset of focal adhesions in the internal region of the cell (see Fig. 1), we selected these adhesions for analysis. Compared to control cells, focal-adhesion assembly was not affected in the coronin-2A-depleted cells (Fig. 3E), but the rate of focal-adhesion disassembly decreased by half (Fig. 3F; supplementary material Movie 2). Together, these data indicate that coronin 2A plays a significant role in controlling disassembly of focal adhesions located at internal regions of the cell.

Adhesion defects caused by the depletion of coronin 2A are mediated through the cofilin pathway

To determine the cause of focal-adhesion turnover defects in the coronin-2A-depleted cells, we examined various cellular pathways and processes that regulate focal-adhesion turnover. There were no significant differences in talin cleavage by calpain, FAK phosphorylation at Y397 or phospho-MLC (*P*-MLC) levels (Fig. 4A). The frequency of microtubule targeting to focal adhesions was decreased in coronin-2A-depleted cells, but this appeared to be caused by slightly decreased microtubule growth rates

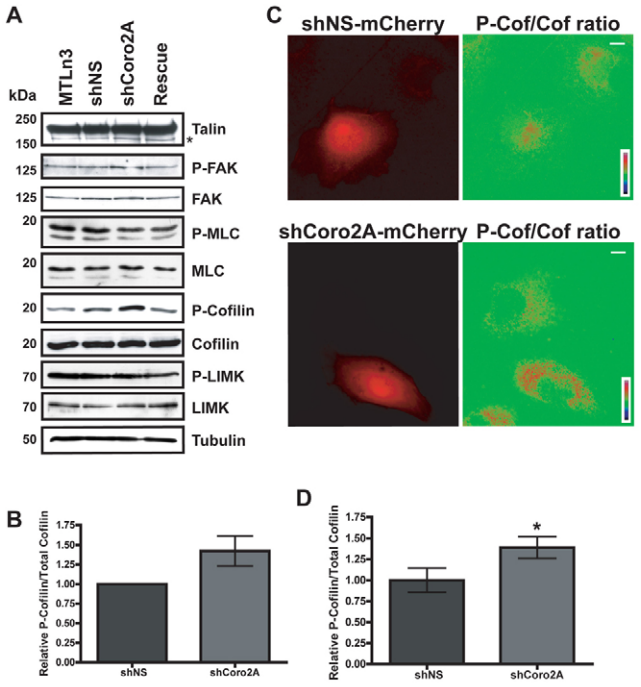

Fig. 4. Depletion of coronin 2A increases *P*-cofilin levels, but has no effect on other focal-adhesion-turnover protein components. (A) Representative immunoblots of MTLn3, shNS, shCoro2A and Rescue cell lysates for talin, *P*-FAK, FAK, *P*-MLC, MLC, *P*-cofilin, cofilin, *P*-LIMK, LIMK and tubulin (loading control). Asterisk indicates calpain-induced talin cleavage product. (B) Quantification of *P*-cofilin versus total cofilin blots. Error bars represent 95% confidence intervals. (C) Representative ratiometric images of *P*-cofilin (P-Cof) and cofilin (Cof) for shNS and shCoro2A cells. Images were normalized to neighboring uninfected cells. Scale bars: 5 µm. (D) Quantification of ratiometric images in C. **P*=0.0001 by Student's *t*-test. Error bars represent 95% confidence intervals.

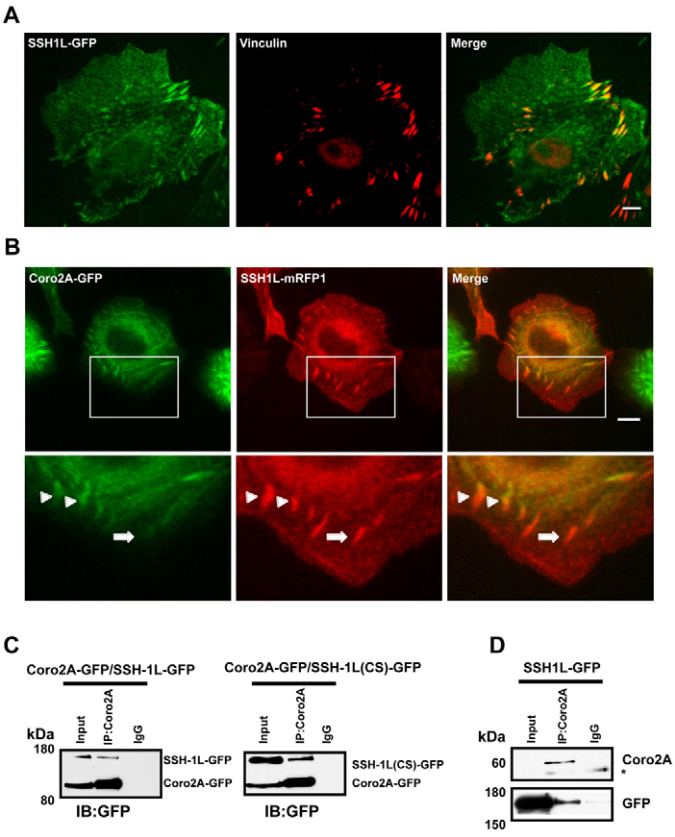

Fig. 5. Coronin 2A interacts with Slingshot-1L and co-localizes at a subset of focal adhesions. (A) SSH1L-GFP localizes to focal adhesions. MTLn3 cells transfected with SSH1L-GFP were fixed and stained with vinculin antibodies. Scale bar: 5 µm. (B) MTLn3 cells expressing Coro2A-GFP and SSH1L-mRFP1 co-localize at focal adhesions. In the lower panel, magnifications (3×) of insets show positive focal adhesions (arrowheads). Some SSH1L-mRFP-positive focal adhesions contain little to no Coro2A-GFP (arrows). (C) Lysates from 293FT cells with enforced expression of Coro2A-GFP and SSH1L-GFP or SSH1L (CS)-GFP were immunoprecipitated with a coronin 2A antibody and immunoblotted for GFP. (D) Co-immunoprecipitation of endogenous coronin 2A with SSH1L-GFP. Immunoprecipitation was performed as for C. Immunoblots were probed with coronin 2A and GFP antibodies. Asterisk indicates antibody immunoglobulin reacting with the secondary antibody.

(supplemental material Fig. S2A,B) and not to be due to microtubule stability or inability to properly target focal adhesions (supplemental material Fig. S2C,D). These observations suggest coronin 2A might control focal-adhesion turnover through a different pathway.

Since coronin 1B regulates cofilin activity at the leading edge of the cell (Cai et al., 2007), we investigated whether coronin 2A has a similar role in regulating cofilin phosphorylation. Depletion of coronin 2A led to roughly a 1.5-fold increase in phosphorylated cofilin (*P*-cofilin) by both western blots (Fig. 4A,B) and ratiometric immunofluorescence (Fig. 4C,D). ADF phosphorylation was also increased in the coronin-2A-depleted cells (supplemental material Fig. S3). To determine whether the increased phosphorylation of cofilin was due to increased LIMK activity in coronin-2A-depleted cells, we blotted for phosphorylated (active) LIMK and observed no change upon depletion of coronin 2A (Fig. 4A). Consistent with a failure to activate LIMK, depletion of coronin 2A did not cause a global change in F-actin content, as measured by changes in phalloidin intensity relative to surrounding control cells (supplemental material Fig. S4).

The cofilin-activating phosphatase Slingshot-1L has been shown to localize to the leading edge of cells and, in agreement with other reports (Soosairajah et al., 2005), we observed Slingshot-1L–GFP (SSH1L-GFP) localizing to focal adhesions (Fig. 5A). Coronin 2A and Slingshot-1L also co-localized at some, but not all, focal adhesions (Fig. 5B). Immunoprecipitations of Coro2A-GFP or endogenous coronin 2A with an antibody against coronin 2A were able to co-immunoprecipitate Slingshot-1L (Fig. 5C,D). This interaction is independent of the phosphatase activity of Slingshot because co-immunoprecipitation occurred with a phosphatase-inactive mutant of Slingshot (CS) equally as well as with wild-type Slingshot (Fig. 5C). Furthermore, endogenous coronin 2A can co-immunoprecipitate with SSH1L-GFP, indicating that this interaction is not mediated by GFP dimerization or by an interaction with GFP (Fig. 5D and control blot in supplemental material Fig. S5).

One obvious mechanism by which coronin 2A might affect the cofilin pathway at focal adhesions is to serve as a targeting subunit for Slingshot-1L at this location. However, SSH1L-GFP targeted focal-adhesion structures equally well in control and coronin-2A-depleted cells (Fig. 6A). Because the depletion of coronin 2A did not appear to affect Slingshot-1L localization to focal adhesions, we examined the dynamics of SSH1L-GFP at focal adhesions in cells expressing either shNS or shCoro2A. The rate of internal focal-adhesion disassembly, as marked by SSH1L-GFP, was similar to

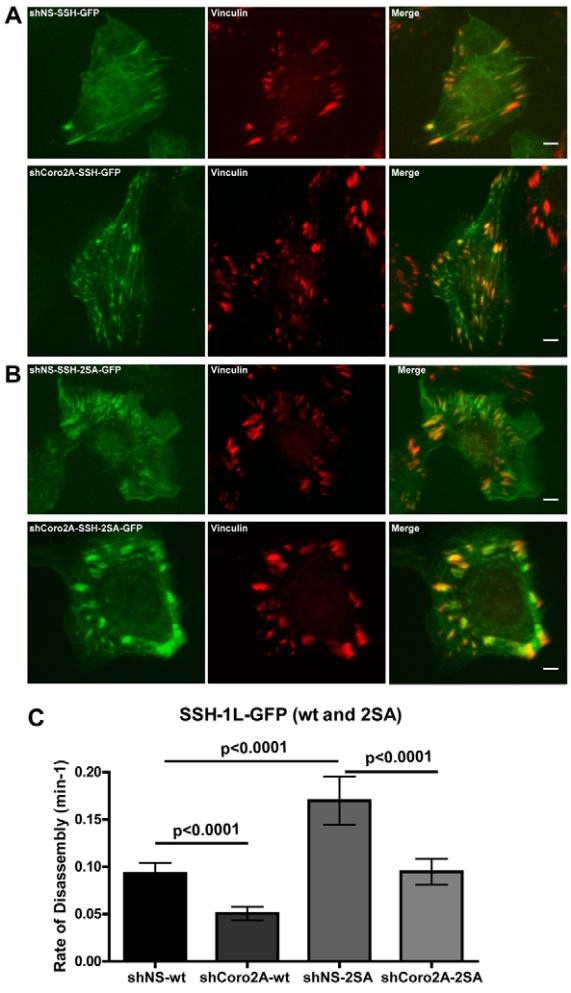

Fig. 6. Active mutants of Slingshot increase focal-adhesion disassembly and partially bypass decreases in focal-adhesion disassembly caused by depletion of coronin 2A. (A) SSH1L-GFP localizes to focal adhesions in cells expressing shNS or shCoro2A. Cells were co-stained with vinculin antibodies. Scale bars: 5 µm. (B) SSH1L-2SA-GFP localizes to focal adhesions in cells expressing shNS or shCoro2A. Cells were co-stained with vinculin antibodies. (C) Focal-adhesion disassembly rates, carried out as for Fig. 3, visualized by SSH1L-GFP or SSH1L-2SA-GFP (active) in cells expressing either shNS or shCoro2A. Error bars represent 95% confidence intervals.

the rate observed with GFP-PXN and displayed the same ~twofold decrease in coronin-2A-depleted cells compared to control cells (Fig. 6C).

Another possibility is that coronin 2A regulates Slingshot-1L activity at focal adhesions. Although Slingshot-1L regulation is incompletely understood, phosphorylation of two serine residues in its C-terminus (S937 and S978) and subsequent 14-3-3 binding have been shown to inhibit its activity (Eiseler et al., 2009; Kligys et al., 2009; Nagata-Ohashi et al., 2004). We examined whether SSH1L-S937A, S978A (abbreviated as SSH1L-2SA), a non-phosphorylatable mutant with higher phosphatase activity, had an effect on focal-adhesion disassembly. Similarly to wild-type Slingshot-1L, SSH1L-2SA–GFP localized to focal adhesions in both control and coronin-2A-depleted cells (Fig. 6B). Expression of the active SSH1L-2SA mutant increased focal-adhesion disassembly rates by ~twofold. Interestingly, depletion of coronin 2A in the cells expressing SSH1L-2SA produced an intermediate result. The rate of disassembly was lower than that with the expression of the mutant alone, but higher than with depletion of coronin 2A in the presence of wild-type Slingshot-1L (Fig. 6C). This result suggests that increased Slingshot activity can compensate for depletion of coronin 2A, but that coronin 2A might also have an effect on focal-adhesion dynamics downstream of Slingshot-1L.

Cofilin localizes to the proximal end of some focal adhesions

Although proteins that regulate cofilin activity, like Slingshot, LIM kinase and TESK, localize to focal adhesions, it remains unclear whether cofilin also localizes to these structures. Cells that were permeabilized with saponin prior to fixation displayed punctate spots of cofilin near the proximal end of some FAK-positive focal adhesions (Fig. 7A), suggesting that endogenous cofilin is stably anchored near some focal adhesions. To circumvent the problem of fixation-induced artifacts, we imaged MTLn3 cells expressing GFP-PXN and cofilin-TagRFP. Live-cell TIRF microscopy showed that spots of cofilin-TagRFP localized to the proximal end of the focal adhesion (Fig. 7B; supplementary material Movie 3). In some cases, the appearance of cofilin at the base of a focal adhesion was followed by focal-adhesion disassembly (Fig. 7B, middle and bottom panels). Although these results suggest that cofilin transiently localizes to some focal adhesions, the precise molecular interactions of cofilin at these structures will require further elucidation in future studies.

Active cofilin can bypass focal-adhesion and motility defects caused by the depletion of coronin 2A

Because cofilin localizes to some focal adhesions, assays were performed to determine whether the severing activity of cofilin occurs at focal adhesions. We used two approaches to evaluate the activity status of cofilin in situ after depletion of coronin 2A. The actin-filament-severing activity of cofilin generates free barbed ends that can be detected by the incorporation of labeled G-actin into permeabilized cells (Chan et al., 2000). Thus, the presence of free barbed ends can be used as a surrogate marker for cofilin activity, although barbed ends at focal adhesions might arise from other mechanisms, such as anti-capping protein activity (e.g. VASP). To measure the density of actin filament barbed ends at focal adhesions, we labeled free barbed ends and visualized them relative to the focal-adhesion marker vinculin. The relative density of free barbed ends at vinculin-positive focal adhesions (reported as the ratio of barbed ends to vinculin staining at focal adhesions) was significantly diminished in coronin-2A-depleted cells (Fig. 8A,B). In addition, fluorescence recovery after photobleaching (FRAP) of TagRFP-actin was performed to monitor any changes in actin dynamics near focal adhesions. Coronin-2A-depleted cells displayed significantly decreased recovery rates of labeled actin at focal adhesions compared to control cells (Fig. 8C). Along with the increased phosphorylation of cofilin in coronin-2A-depleted cells, reduced density of barbed ends at focal adhesions, and the interaction of coronin 2A and Slingshot-1L, these data suggest that coronin 2A enhances disassembly of a subset of internal focal adhesions through the cofilin pathway.

To directly determine whether decreased cofilin activity is responsible for the decreased cell motility in the coronin-2A-depleted cells, we tested whether an active mutant of cofilin (cofilin S3A) could bypass these defects. Expression of cofilin S3A in coronin-2A-depleted cells restored whole-cell motility to that of control cells (Fig. 9A). To test whether the defect in focal-adhesion

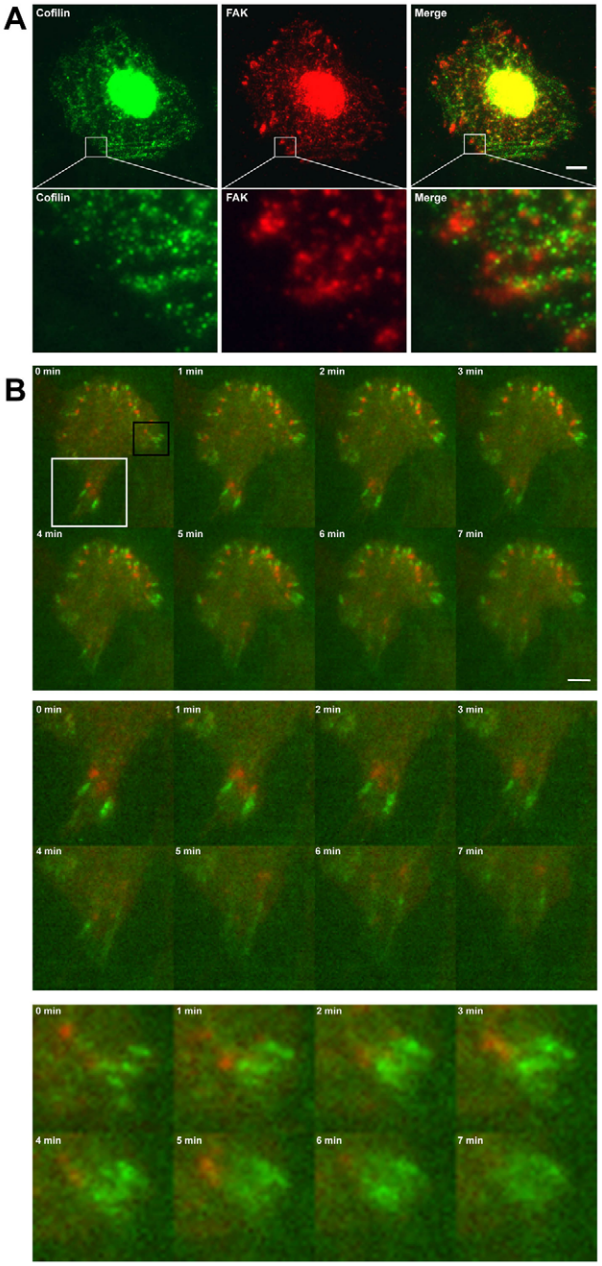

Fig. 7. Cofilin localizes to the proximal end of some focal adhesions in fixed and live cells. (A) Immunofluorescent images of saponin-permeabilized MTLn3 cells stained for cofilin and FAK. Lower panel shows magnifications (7.5×) of insets. Scale bar: 5 µm. (B) Montage of live-cell images of cell expressing shNS-GFP-PXN and cofilin-TagRFP. Images were taken every minute (see supplementary material Movie 3). Scale bar: 5 µm. Cofilin-TagRFP localizes to the base of GFP-PXN-positive focal adhesions, leading to focal-adhesion disassembly. Middle panel gives enlarged (2.2×) view of white box inset. Bottom panel gives enlarged (4.3×) view of black box inset.

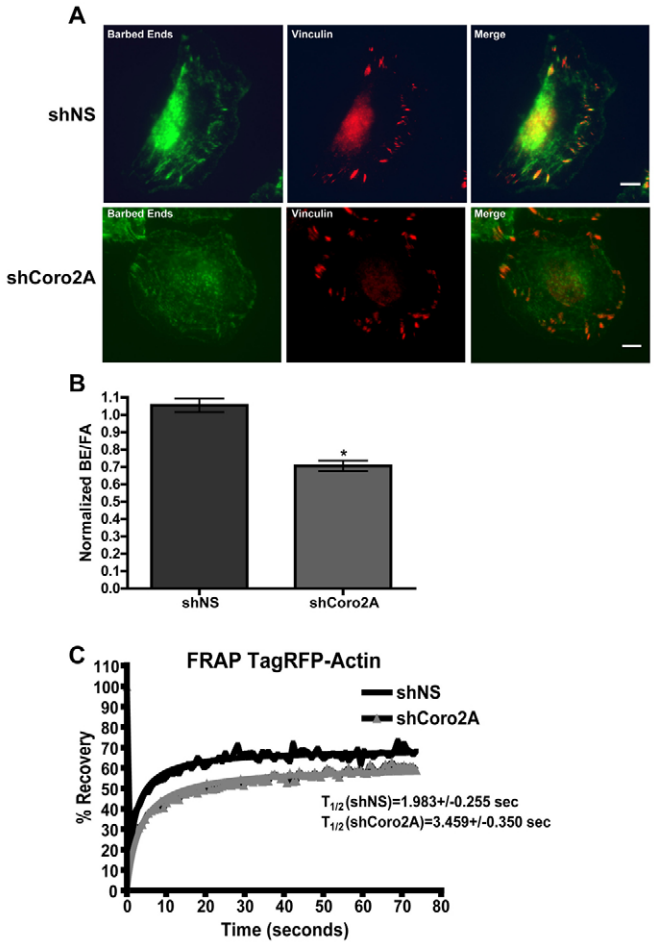

Fig. 8. Depletion of coronin 2A leads to reduced barbed-end density and actin turnover at internal focal adhesions. (A) Representative images of Oregon green actin conjugate incorporated into free barbed ends at vinculin-stained focal adhesions in MTLn3 cells expressing shNS-TagRFP-actin or shCoro2A-TagRFP-actin. Scale bars: 5 µm. (B) Graph depicting the ratio of barbed ends to focal adhesions (BE/FA), as measured by average fluorescence intensities. These results were normalized to the intensity values of uninfected MTLn3 cells on the same coverslip. Error bars indicate 95% confidence intervals. *P<0.001 by Student's t-test. (C) Graph of fluorescence recovery after photobleaching (FRAP) of TagRFP-actin at focal adhesions in MTLn3 cells expressing either shNS or shCoro2A. $T_{1/2}$ values indicate time required for 50% recovery of fluorescence. Values from nine cells were used to calculate the recovery rate.

turnover present in the coronin-2A-depleted cells was due to insufficient cofilin activity, we expressed either wild-type or cofilin S3A in the coronin-2A-depleted cells. Expression of the wild-type cofilin was unable to rescue the defect in internal focal-adhesion disassembly observed with depletion of coronin 2A (Fig. 9B). However, expression of cofilin S3A in coronin-2A-depleted cells restored internal focal-adhesion disassembly rates to the rate of control cells (Fig. 9B). Expression of cofilin S3A alone had no effect on whole-cell motility or focal-adhesion turnover, suggesting that the bypass effect of this mutant is specific to depletion of coronin 2A. Together, these data indicate that coronin 2A affects focal-adhesion disassembly through the activation of cofilin.

Discussion

Considerable evidence points to the important role that coronins play in cell motility, but the function of type II coronins, such as coronin 2A, has never been addressed. Unlike the more well-characterized type I coronins, coronin 2A localizes to stress fibers and some focal adhesions, and is excluded from the leading edge. Our data indicate that coronin 2A plays a key role in regulating whole-cell motility and internal focal-adhesion turnover. Depletion of this gene leads to insufficient cofilin activity at focal adhesions

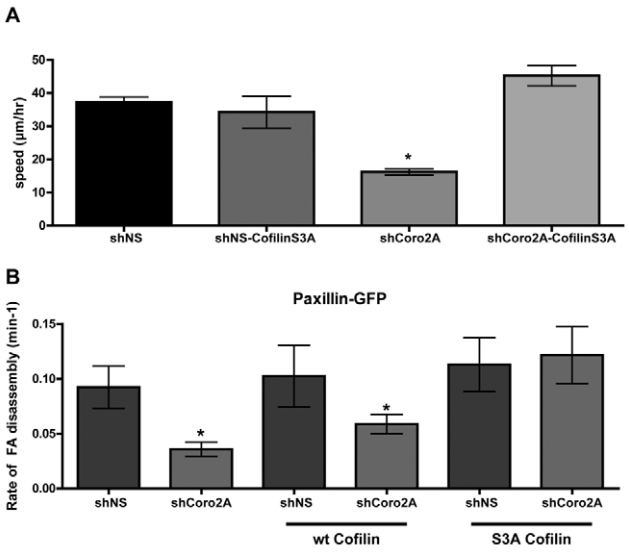

Fig. 9. Expression of cofilin S3A rescues cell motility and focal-adhesion disassembly defects caused by depletion of coronin 2A. (A) Graph of average cell speeds of MTLn3, shNS, shCoro2A, shNS-cofilinS3A and shCoro2A-cofilinS3A expressing cells, as done in Fig. 2. Error bars indicate 95% confidence intervals. Asterisk indicates $P<0.001$. (B) Graph of average rates of focal adhesion (FA) disassembly visualized by GFP-PXN in cells expressing either shNS or shCoro2A along with wild-type (wt) or S3A cofilin-mRFP1, as done in Fig. 3. Error bars indicate 95% confidence intervals. *$P<0.001$ by Student's *t*-test.

and reduced adhesion disassembly in the interior region of the cell. This effect might be mediated in part through a coronin-2A–Slingshot-1L interaction that regulates Slingshot (and therefore cofilin) activity. Consistent with a role of cofilin activation in these processes, defects in motility and internal focal-adhesion turnover induced by depletion of coronin 2A can be bypassed by an active mutant of cofilin.

Our data highlight the striking diversity of localization and function in the mammalian coronin family of proteins. Previous data from our laboratory indicate that the primary function of type I coronins (e.g. coronin 1B) is to interact with the Arp2/3 complex and Slingshot-1L at the rear of the lamellipodia and remodel the dendritic meshwork (Cai et al., 2007; Cai et al., 2008). Like coronin 1B, coronin 2A interacts with Slingshot-1L. This indicates that cofilin regulatory activity is conserved between type I and II coronins. Despite this similarity, type I coronins and coronin 2A have distinct spatial distributions. Coronin 2A localizes to stress fibers and focal adhesions in the central region of the cell and is excluded from the leading edge, whereas type I coronins are concentrated in this compartment. It remains unclear what causes these differences in localization patterns, and elucidating this will require further investigation.

A significant conclusion from these studies is that activation of the severing activity of cofilin is an important factor in a subset of focal-adhesion-disassembly events. Previous studies on TESK1 have shown a requirement of cofilin phosphorylation for proper spreading to occur, but did not address the role of cofilin in regulating focal-adhesion dynamics (LaLonde et al., 2005). Although many studies have linked cofilin activity to actin turnover at specific structures, such as the dendritic meshwork, stress fibers and myofibril arrays (Ono, 2007), our data are the first to directly implicate cofilin activity in the turnover of focal adhesions. One simple model for the direct involvement of cofilin in this process is that actin filaments in stress fibers connected to focal adhesions must be severed to initiate, propagate or complete the turnover of the adhesion. Data from others has already indicated that the linkage between stress fibers and focal-adhesion components, such as PXN, is capable of slipping in a clutch-like fashion (Hu et al., 2007). Thus, severing by cofilin might reflect an alternate pathway by which the linkage between stress fibers and focal adhesions can be regulated. Since some studies have indicated that cofilin poorly severs actin filaments in bundled structures (Michelot et al., 2007), there might be a requirement for bundle remodeling near the point of cofilin action in order for this mechanism to function efficiently.

One intriguing issue that arises from these studies is that of how coronin 2A modulates cofilin activity at focal adhesions. On the basis of the increased levels of *P*-cofilin observed with coronin 2A depletion and the selective ability of cofilin S3A (but not wild-type) to bypass the motility and adhesion turnover defects, it seems probable that coronin 2A affects cofilin activity, at least in part, via its phosphorylation status. The interaction between coronin 2A and Slingshot-1L supports this notion, but it is important to point out that coronin 2A does not simply target Slingshot-1L to focal adhesions. Furthermore, coronin 2A is unlikely to exclusively regulate Slingshot-1L activity through controlling the phosphorylation of the C-terminal serine residues because the enhanced focal-adhesion disassembly caused by expression of the activated Slingshot-1L 2SA mutant would have been completely unaffected by depletion of coronin 2A in this case. Thus, coronin 2A might control Slingshot-1L activity by an unknown mechanism. Alternately, coronin 2A might affect cofilin by a Slingshot-1L-independent mechanism, such as through an effect on the structure of actin filaments in the focal adhesion, or through the direct enhancement of cofilin activity, as described recently for coronin 1A in an in vitro system (Kueh et al., 2008). These and other possibilities will need to be addressed in future experiments.

Previous studies uncovered multiple mechanisms for focal-adhesion turnover and it is worth considering how cofilin-based severing might be integrated with some of these other mechanisms. One significant mechanism of turnover is the calpain-dependent cleavage of talin (Huttenlocher et al., 1997; Bhatt et al., 2002). This event permanently breaks a key linkage between integrin receptors and other components in the focal-adhesion plaque. Cofilin-based severing of actin filaments might serve a similar purpose at the proximal end of the focal adhesion and might synergistically accelerate adhesion turnover. Another important mechanism of adhesion assembly and disassembly is myosin-based contractility. The isometric tension generated by this mechanism is important for the maturation of nascent contacts near the leading edge and is also important for detachment of adhesions at the trailing edge (Rottner et al., 1999; Webb et al., 2004; Gupton and Waterman-Storer, 2006). Cofilin-based severing could directly impact myosin-based contractility by modifying actin filament structure near the adhesion. It is unclear how these mechanisms and others such as microtubule contact and FAK-dynamin interactions function together to drive focal-adhesion turnover.

In addition to the complication of multiple interrelated mechanisms of focal-adhesion turnover, it is clear that different mechanisms might dominate in particular cellular compartments and in different cell types. Cells must balance the formation and dissolution of adhesions in an asymmetric manner to promote efficient cell migration. Thus, adhesion turnover at the front of the

cells might utilize a distinct set of turnover mechanisms from those at the trailing edge of the cells. Because coronin 2A is excluded from the periphery of the cell, it seems likely that it would participate only in turnover of centrally located adhesions. Finally, it is important to note that expression of coronin 2A is not detectable in fibroblasts and thus its role in focal-adhesion turnover might be specific for certain cell types such as epithelial cells. However, various Slingshot and LIMK isoforms are ubiquitously expressed, so regulated cofilin activation might be an intrinsic part of focal-adhesion turnover in all cells. Considering the profound effect that focal-adhesion-turnover kinetics has on overall cell migration, it will be crucial to elucidate this process in detail in order to fully understand migration-dependent processes such as the immune response and cancer metastasis.

Materials and Methods

Molecular cloning

pML2 (human Coro2A-GFP) has been described previously (Cai et al., 2005). Rat coronin 2A was amplified from cDNA made from MTLn3 cells. pLL5.0 base vector and pLL5.0-shNS-GFP/mCherry have been described (Cai et al., 2007). shRNA sequences were designed to target rat, but not human, coronin 2A (shCoro2A). Oligonucleotides were annealed and ligated in HpaI and XhoI sites in pLL5.0. The coronin 2A shRNA sequence is 5′-GGAACGTCTTGGACATCAT-3′. A rescue construct was made by PCR amplification of human coronin 2A and cloning it into EcoRI and BamHI sites in pLL5.0-shCoro2A. The following cDNAs were PCR amplified and inserted in pLL5.0-shNS-GFP and pLL5.0-shCoro2A-GFP with the sites indicated: paxillin (GFP-PXN; double blunt ligation into RI/SbfI site), Slingshot-1L (wt or CS) (SSH1L-GFP; MfeI/BglII into EcoRI/BamHI in pLL5.0), cofilin A (EcoRI/BamHI) and TagRFP-actin (EcoRI/SbfI). cDNAs for SSH1L and cofilin S3A were PCR amplified, digested with SalI/SacII or EcoRI/BamHI, respectively, and ligated into pML2-mRFP1. SSH1L-2SA-GFP was made by site-directed mutation of serine 937 and serine 978 to alanines. PCR primers sequences are available upon request.

Antibodies and reagents

GST-coronin 2A short tail (human, amino acids 493-526) was produced in *Escherichia coli*, purified using glutathione-Agarose beads, and used to inject rabbits for the production of polyclonal antibodies for coronin 2A (Covance). Purified antibodies were isolated by applying serum to MBP-coronin 2A short tail that was immobilized on an UltraLink Biosupport (Pierce). Antibodies were eluted from the column with both high and low pH solutions and tested for recognition of coronin 2A protein by immunoblotting (WB), immunofluorescence (IF) and immunoprecipitation (IP). The following antibodies were purchased and used at the dilutions as indicated: α-tubulin clone DM1A (Sigma; WB 1:1000), GFP clone JL-8 (Clontech; WB 1:5000) or (Roche; IP 1 μl), talin (Sigma; WB 1:5000), FAK [Millipore; WB 1:1000, IF 1:200, or BC3 (a gift from Mike Schaller, University of West Virginia, Morgantown, WV), IF 1:200], *P*-FAK (Biosource; WB 1:1000), cofilin (Cytoskeleton; WB 1:500) or [Mab22 (a gift from Jim Bamburg, Colorado State University, Fort Collins, CO) IF 1:100], *P*-cofilin [Biosource, WB 1:1000, or 4321 (a gift from Jim Bamburg), IF 1:70)], LIMK (Cell Signaling; WB 1:1000), *P*-LIMK (ECM Biosciences; WB 1:1000), MLC II (Cell Signaling; WB 1:1000), and *P*-MLC (Cell Signaling; WB 1:1000). Coronin 1B rabbit polyclonal antibody is described in the literature (Cai et al., 2005). Cy2, Cy5, rhodamine red-X, and HRP conjugated secondary antibodies were from Jackson ImmunoResearch Laboratories. Immobilon-P PVDF was from Millipore. Recombinant Rat EGF was purchased from Sigma. Rat tail collagen was purchased from BD Biosciences. 100× Pen Strep glutamine (PSG), α-MEM, DMEM, Alexa Fluor 488, 568 and 647 labeled with phalloidin, Oregon green and Alexa Fluor 647 actin conjugates were purchased from Invitrogen. Fetal bovine serum (FBS) was purchased from Hyclone.

Cell Culture and shRNA lentiviral production

MTLn3 cells (a gift from John Condeelis, Albert Einstein College of Medicine, Bronx, NY), a rat mammary adenocarcinoma cell line described by Chan et al. (Chan et al., 1998), were grown in α-MEM containing 5% FBS and 1× PSG. 293FT cells were grown in DMEM containing 10% FBS and 1× PSG. Retroviral and lentiviral production was preformed as previously described (Cai et al., 2007). MTLn3 cells were infected with retrovirus or lentivirus for 4 hours and then the media was changed. Effects of lentiviral infections were examined by western blot after 3-4 days.

ACEA RT-CES experiments

After background measurements were taken (100 μl of media), 5000 cells in 100 μl was added to each well (three experiments, done in triplicate). Impedance measurements were taken every 2 minutes for 3 hours and quantified in Prism (Graph Pad)

Single cell tracking

MTLn3 cells were either uninfected or infected with lentiviruses encoding shNS, shCoro2A, rescue, shNS–cofilin-S3A–GFP or shCoro2A–cofilin-S3A–GFP. These cells were plated on 50 μg/ml rat tail collagen-coated Bioptechs Delta T dishes for 16-18 hours. Time-lapse microscopy was performed on an Olympus IX-81 inverted microscope (10× objective) with a Hamamatsu CCD camera (model c4742-80-12AG). Cell speed was measured with Tracking software (Andor Bioimaging) or Slidebook software (Intelligent Imaging Innovations) using manual tracking mode. Graphs displayed were made in Prism (Graph-Pad).

Immunoprecipitations

293FT cells were transfected with plasmids as indicated in the figures. An 80-90% confluent 6-cm dish of cells was lysed in 1 ml of 1% Triton X-100 in PBS. Lysates were spun at 16,873 ***g*** at 4°C for 5 minutes. Approximately 1 μg of GFP or coronin 2A antibodies were used for immunoprecipitation in combination with 20 μl of protein A or protein-G Sepharose beads (Pierce or GE Lifesciences, respectively). Immunoprecipitated proteins were separated by SDS-PAGE, transferred to PVDF (Millipore), and immunoblotted for coronin 2A or GFP.

Focal-adhesion-assembly and -disassembly experiments

MTLn3 cells infected with shNS-GFP-PXN, shCoro2A-GFP-PXN, shNS-SSH1L-GFP, shCoro2A-SSH1L-GFP, shNS-SSH1L-2SA-GFP, or shCoro2A-SSH1L-2SA-GFP were plated as in single-cell tracking experiments. Cells were imaged on a Nipkow-type spinning disk confocal scan head (Yokogawa CSU-10) with a 60× 1.45 NA objective. Images were taken 1 frame every minute for 40 minutes. In four cells over two experiments, at least 12 focal adhesions per cell were analyzed with ImageJ software. These adhesions fit the criteria that they were not (1) localized to the edge of a protruding lamellipodia, and (2) localized to either the tail or internal region of the cell. The intensity of GFP in each frame was used to determine rates of focal-adhesion assembly and disassembly as described (Webb et al., 2004). All images were corrected for photobleaching.

Focal-adhesion and cofilin live-cell imaging

MTLn3 cells infected with shNS-GFP-PXN and cofilin-TagRFP were plated as in focal-adhesion-assembly and -disassembly conditions. Total internal reflectance microscopy (Olympus) was used to illuminate fluorescent proteins in close proximity to the coverslip. Images of cofilin and PXN were taken every minute for 30 minutes.

Immunofluorescence

MTLn3 cells were plated on acid-washed coverslips coated with 50 μg/ml rat tail collagen. Cells were fixed with 4% PFA, or pre-permeabilized in permeabilization buffer (20 mM Hepes at pH 7.5, 138 mM KCl, 4 mM MgCl2, 3 mM EGTA, 0.2 mg/ml saponin, 1 mM ATP, 1% BSA) for 30 seconds followed by 4% PFA fixation for 10 minutes. After three washes with PBS, cells were permeabilized with 0.1% Triton X-100 in PBS for 5 minutes. Cells were blocked for 15 minutes in PBS containing 5% normal goat serum (Jackson Laboratories) and 5% fatty-acid-free BSA. Primary antibodies were applied to cells in PBS containing 1% BSA for 1 hour. If needed, diluted primary antibody solutions also contained Alexa Fluor 488, 568, or 647 phalloidin (Invitrogen). Cells were washed three times in PBS. Cy2, Cy5 and rhodamine red-X conjugated secondary antibodies were diluted to 1:400 in 1% BSA in PBS and applied to the coverslips for 1 hour. After three washes in PBS, the coverslips were mounted onto slides with Fluoromount G (Electron Microscopy Sciences). Barbed-end experiments were carried out as described (Chan et al., 2000). Briefly, cells were permeabilized in permeabilization buffer containing 2 μM Oregon green or Alexa Fluor 647 actin conjugates (Invitrogen) for 20 seconds. Cells were then fixed and processed as above.

Fluorescence recovery after photobleaching

MTLn3 cells infected with shNS-TagRFP-actin or shCoro2A-TagRFP-actin were photobleached at focal adhesions with a 405-nm laser for 30 milliseconds. TagRFP fluorescence intensities were monitored every 0.784 seconds on an Olympus FV1000 microscope with a 60× 1.2NA Olympus objective. Nine cells were analyzed for each condition. All images were corrected for overall photobleaching. Images were analyzed in ImageJ.

Ratiometric imaging of *P*-cofilin and cofilin

MTLn3 cells were fixed with 4% PFA and processed as in the immunofluorescence experiments. Fields containing both an infected cell expressing either shNS or shCoro2A-mCherry and an uninfected cell were imaged in the linear range of the camera. Fluorescent images of *P*-cofilin and cofilin were collected and processed using the ImageJ plug-in Ratio plus. Relative intensities were obtained by normalizing the values to the uninfected neighboring cells for 30 cells per treatment.

EB1-GFP experiments

MTLn3 cells expressing either shNS-EB1-GFP or shCoro2A-EB1-GFP with or without TagRFP-actin were imaged either every second for EB1-GFP dynamics and microtubule growth rate studies, or every 3 seconds for focal-adhesion targeting. Focal-adhesion targeting was determined by EB1-GFP tracking down an actin stress fiber and terminating at the base of the stress fiber (considered to be a targeting event). EB1-GFP velocity (rate of microtubule growth) was determined by tracking the centroid of the EB1-GFP spot over time. The distance divided by time was used to determine EB1 velocity. Growth phase was determined to be the amount of time an EB1-GFP spot is observed over the course of a movie. Because EB1-GFP localization requires a growing microtubule, this was used to estimate microtubule stability.

We would like to thank Keith Burridge, Alan Fanning and David Roadcap for critical reading of the manuscript, Erika Whittchen for help with the ACEA system, and Jim Bamburg, John Condeelis and Mike Schaller (University of West Virginia, Morgantown, WV) for generous gifts of reagents. This work was supported by grants from NIH (GM083035), ACS (RSG-08-154-01) and the Sontag Foundation. Deposited in PMC for release after 12 months.

References

Bamburg, J. R. and Bernstein, B. W. (2008). ADF/cofilin. *Curr. Biol.* **18**, R273-R275.

Bhatt, A., Kaverina, I., Otey, C. and Huttenlocher, A. (2002). Regulation of focal complex composition and disassembly by the calcium-dependent protease calpain. *J. Cell Sci.* **115**, 3415-3425.

Cai, L., Holoweckyj, N., Schaller, M. D. and Bear, J. E. (2005). Phosphorylation of coronin 1B by protein kinase C regulates interaction with Arp2/3 and cell motility. *J. Biol. Chem.* **280**, 31913-31923.

Cai, L., Marshall, T. W., Uetrecht, A. C., Schafer, D. A. and Bear, J. E. (2007). Coronin 1B coordinates Arp2/3 complex and cofilin activities at the leading edge. *Cell* **128**, 915-929.

Cai, L., Makhov, A. M., Schafer, D. A. and Bear, J. E. (2008). Coronin 1B antagonizes cortactin and remodels Arp2/3-containing actin branches in lamellipodia. *Cell* **134**, 828-842.

Chan, A. Y., Raft, S., Bailly, M., Wyckoff, J. B., Segall, J. E. and Condeelis, J. S. (1998). EGF stimulates an increase in actin nucleation and filament number at the leading edge of the lamellipod in mammary adenocarcinoma cells. *J. Cell Sci.* **111**, 199-211.

Chan, A. Y., Bailly, M., Zebda, N., Segall, J. E. and Condeelis, J. S. (2000). Role of cofilin in epidermal growth factor-stimulated actin polymerization and lamellipod protrusion. *J. Cell Biol.* **148**, 531-542.

de Hostos, E. L., Rehfuess, C., Bradtke, B., Waddell, D. R., Albrecht, R., Murphy, J. and Gerisch, G. (1993). Dictyostelium mutants lacking the cytoskeletal protein coronin are defective in cytokinesis and cell motility. *J. Cell Biol.* **120**, 163-173.

Eiseler, T., Doppler, H., Yan, I. K., Kitatani, K., Mizuno, K. and Storz, P. (2009). Protein kinase D1 regulates cofilin-mediated F-actin reorganization and cell motility through slingshot. *Nat. Cell Biol.* **11**, 545-556.

Ezratty, E. J., Partridge, M. A. and Gundersen, G. G. (2005). Microtubule-induced focal adhesion disassembly is mediated by dynamin and focal adhesion kinase. *Nat. Cell Biol.* **7**, 581-590.

Foger, N., Rangell, L., Danilenko, D. M. and Chan, A. C. (2006). Requirement for coronin 1 in T lymphocyte trafficking and cellular homeostasis. *Science* **313**, 839-842.

Foletta, V. C., Moussi, N., Sarmiere, P. D., Bamburg, J. R. and Bernard, O. (2004). LIM kinase 1, a key regulator of actin dynamics, is widely expressed in embryonic and adult tissues. *Exp. Cell Res.* **294**, 392-405.

Franco, S. J., Rodgers, M. A., Perrin, B. J., Han, J., Bennin, D. A., Critchley, D. R. and Huttenlocher, A. (2004). Calpain-mediated proteolysis of talin regulates adhesion dynamics. *Nat. Cell Biol.* **6**, 977-983.

Frantz, C., Barreiro, G., Dominguez, L., Chen, X., Eddy, R., Condeelis, J., Kelly, M. J., Jacobson, M. P. and Barber, D. L. (2008). Cofilin is a pH sensor for actin free barbed end formation: role of phosphoinositide binding. *J. Cell Biol.* **183**, 865-879.

Gohla, A., Birkenfeld, J. and Bokoch, G. M. (2005). Chronophin, a novel HAD-type serine protein phosphatase, regulates cofilin-dependent actin dynamics. *Nat. Cell Biol.* **7**, 21-29.

Gupton, S. L. and Waterman-Storer, C. M. (2006). Spatiotemporal feedback between actomyosin and focal-adhesion systems optimizes rapid cell migration. *Cell* **125**, 1361-1374.

Hagel, M., George, E. L., Kim, A., Tamimi, R., Opitz, S. L., Turner, C. E., Imamoto, A. and Thomas, S. M. (2002). The adaptor protein paxillin is essential for normal development in the mouse and is a critical transducer of fibronectin signaling. *Mol. Cell. Biol.* **22**, 901-915.

Hotulainen, P., Paunola, E., Vartiainen, M. K. and Lappalainen, P. (2005). Actin-depolymerizing factor and cofilin-1 play overlapping roles in promoting rapid F-actin depolymerization in mammalian nonmuscle cells. *Mol. Biol. Cell* **16**, 649-664.

Hu, K., Ji, L., Applegate, K. T., Danuser, G. and Waterman-Storer, C. M. (2007). Differential transmission of actin motion within focal adhesions. *Science* **315**, 111-115.

Huttenlocher, A., Palecek, S. P., Lu, Q., Zhang, W., Mellgren, R. L., Lauffenburger, D. A., Ginsberg, M. H. and Horwitz, A. F. (1997). Regulation of cell migration by the calcium-dependent protease calpain. *J. Biol. Chem.* **272**, 32719-32722.

Ilic, D., Furuta, Y., Kanazawa, S., Takeda, N., Sobue, K., Nakatsuji, N., Nomura, S., Fujimoto, J., Okada, M. and Yamamoto, T. (1995). Reduced cell motility and enhanced focal adhesion contact formation in cells from FAK-deficient mice. *Nature* **377**, 539-544.

Katz, M., Amit, I., Citri, A., Shay, T., Carvalho, S., Lavi, S., Milanezi, F., Lyass, L., Amariglio, N., Jacob-Hirsch, J. et al. (2007). A reciprocal tensin-3-cten switch mediates EGF-driven mammary cell migration. *Nat. Cell Biol.* **9**, 961-969.

Kaverina, I., Krylyshkina, O. and Small, J. V. (1999). Microtubule targeting of substrate contacts promotes their relaxation and dissociation. *J. Cell Biol.* **146**, 1033-1044.

Kligys, K., Yao, J., Yu, D. and Jones, J. C. (2009). 14-3-3zeta/tau heterodimers regulate Slingshot activity in migrating keratinocytes. *Biochem. Biophys. Res. Commun.* **383**, 450-454.

Kueh, H. Y., Charras, G. T., Mitchison, T. J. and Brieher, W. M. (2008). Actin disassembly by cofilin, coronin, and Aip1 occurs in bursts and is inhibited by barbed-end cappers. *J. Cell Biol.* **182**, 341-353.

Lahlou, H., Sanguin-Gendreau, V., Zuo, D., Cardiff, R. D., McLean, G. W., Frame, M. C. and Muller, W. J. (2007). Mammary epithelial-specific disruption of the focal adhesion kinase blocks mammary tumor progression. *Proc. Natl. Acad. Sci. USA* **104**, 20302-20307.

LaLonde, D. P., Brown, M. C., Bouverat, B. P. and Turner, C. E. (2005). Actopaxin interacts with TESK1 to regulate cell spreading on fibronectin. *J. Biol. Chem.* **280**, 21680-21688.

Michelot, A., Berro, J., Guerin, C., Boujemaa-Paterski, R., Staiger, C. J., Martiel, J. L. and Blanchoin, L. (2007). Actin-filament stochastic dynamics mediated by ADF/cofilin. *Curr. Biol.* **17**, 825-833.

Mitra, S. K. and Schlaepfer, D. D. (2006). Integrin-regulated FAK-Src signaling in normal and cancer cells. *Curr. Opin. Cell Biol.* **18**, 516-523.

Nagata-Ohashi, K., Ohta, Y., Goto, K., Chiba, S., Mori, R., Nishita, M., Ohashi, K., Kousaka, K., Iwamatsu, A., Niwa, R. et al. (2004). A pathway of neuregulin-induced activation of cofilin-phosphatase Slingshot and cofilin in lamellipodia. *J. Cell Biol.* **165**, 465-471.

Nakamura, T., Takeuchi, K., Muraoka, S., Takezoe, H., Takahashi, N. and Mori, N. (1999). A neurally enriched coronin-like protein, ClipinC, is a novel candidate for an actin cytoskeleton-cortical membrane-linking protein. *J. Biol. Chem.* **274**, 13322-13327.

Niwa, R., Nagata-Ohashi, K., Takeichi, M., Mizuno, K. and Uemura, T. (2002). Control of actin reorganization by Slingshot, a family of phosphatases that dephosphorylate ADF/cofilin. *Cell* **108**, 233-246.

Ono, S. (2007). Mechanism of depolymerization and severing of actin filaments and its significance in cytoskeletal dynamics. *Int. Rev. Cytol.* **258**, 1-82.

Rosentreter, A., Hofmann, A., Xavier, C. P., Stumpf, M., Noegel, A. A. and Clemen, C. S. (2007). Coronin 3 involvement in F-actin-dependent processes at the cell cortex. *Exp. Cell Res.* **313**, 878-895.

Rottner, K., Hall, A. and Small, J. V. (1999). Interplay between Rac and Rho in the control of substrate contact dynamics. *Curr. Biol.* **9**, 640-648.

Rybakin, V., Stumpf, M., Schulze, A., Majoul, I. V., Noegel, A. A. and Hasse, A. (2004). Coronin 7, the mammalian POD-1 homologue, localizes to the Golgi apparatus. *FEBS Lett.* **573**, 161-167.

Sidani, M., Wessels, D., Mouneimne, G., Ghosh, M., Goswami, S., Sarmiento, C., Wang, W., Kuhl, S., El-Sibai, M., Backer, J. M. et al. (2007). Cofilin determines the migration behavior and turning frequency of metastatic cancer cells. *J. Cell Biol.* **179**, 777-791.

Soosairajah, J., Maiti, S., Wiggan, O., Sarmiere, P., Moussi, N., Sarcevic, B., Sampath, R., Bamburg, J. R. and Bernard, O. (2005). Interplay between components of a novel LIM kinase-slingshot phosphatase complex regulates cofilin. *EMBO J.* **24**, 473-486.

Toshima, J., Toshima, J. Y., Amano, T., Yang, N., Narumiya, S. and Mizuno, K. (2001). Cofilin phosphorylation by protein kinase testicular protein kinase 1 and its role in integrin-mediated actin reorganization and focal adhesion formation. *Mol. Biol. Cell* **12**, 1131-1145.

Uetrecht, A. C. and Bear, J. E. (2006). Coronins: the return of the crown. *Trends Cell Biol.* **16**, 421-426.

van Rheenen, J., Song, X., van Roosmalen, W., Cammer, M., Chen, X., Desmarais, V., Yip, S. C., Backer, J. M., Eddy, R. J. and Condeelis, J. S. (2007). EGF-induced PIP2 hydrolysis releases and activates cofilin locally in carcinoma cells. *J. Cell Biol.* **179**, 1247-1259.

Webb, D. J., Donais, K., Whitmore, L. A., Thomas, S. M., Turner, C. E., Parsons, J. T. and Horwitz, A. F. (2004). FAK-Src signalling through paxillin, ERK and MLCK regulates adhesion disassembly. *Nat. Cell Biol.* **6**, 154-161.

Yang, N., Higuchi, O., Ohashi, K., Nagata, K., Wada, A., Kangawa, K., Nishida, E. and Mizuno, K. (1998). Cofilin phosphorylation by LIM-kinase 1 and its role in Rac-mediated actin reorganization. *Nature* **393**, 809-812.